Fluorescence Study of the Solvation of Fluorescent Probes Prodan and Laurdan in Poly(ϵ-caprolactone)-*block*-poly(ethylene oxide) Vesicles in Aqueous Solutions with Tetrahydrofurane

Radek Šachl, Miroslav Štěpánek,* and Karel Procházka*

Department of Physical and Macromolecular Chemistry, Faculty of Science, Charles University in Prague, Hlavova 2030, 128 40 Prague 2, Czech Republic

Jana Humpolíčková and Martin Hof

Jaroslav Heyrovský Institute of Physical Chemistry of the Academy of Sciences of the Czech Republic, Dolejškova 3, 182 23 Prague 8, Czech Republic

Received August 9, 2007. In Final Form: October 11, 2007

Steady-state and time-resolved fluorescence measurements were used to study the relaxation of the microenvironment of hydrophobic probes 6-propionyl-2-(dimethylamino)naphthalene (prodan) and 6-dodecanoyl-2-(dimethylamino)-naphthalene (laurdan) in systems containing vesicles formed by the amphiphilic diblock copolymer poly(ϵ-caprolactone)-*block*-poly(ethylene oxide) (PCL-PEO) and water/tetrahydrofurane (THF) solvent mixtures. It was found that in case of prodan, both steady-state and time-resolved emission spectra were composed of two subspectra corresponding to the emission of prodan molecules located (i) in fairly rigid (effectively viscous) and hydrophobic domains of the vesicles close to the PCL/PEO interface and (ii) in a more polar and less viscous medium (in the bulk solution). The fraction of the emission from the more polar microenvironment increases with increasing content of THF in the system. Laurdan, in contrast to prodan, appeared to be solubilized preferentially in the hydrophobic domains up to 30 vol % of THF content, and its emission spectra changed only due to swelling of hydrophobic PCL domains by added THF. The study shows that the analysis of the time-resolved emission from a probe distributed in two media is, in principle, possible, but it is quite complex and appreciably less accurate, and the relaxation times are ill-defined averages of several processes. The bimodal or shoulder-containing time-resolved spectra have to be decomposed in pertinent time-resolved subspectra and treated separately. Another important result of the study is a piece of knowledge concerning the motion of the probe with respect to the vesicle. In the studied complex system, not only the relaxation of the solvent and reorganization of polymer segments around the fluorescent headgroup of the probe affect the emission but also a lateral motion of the probe with respect to the nanoparticle within the lifetime of the excited state contributes significantly to the relaxation and to the relatively slow time-resolved Stokes shift.

Introduction

Fluorescence emission is very sensitive to the interplay of the excited fluorophore with its microenvironment (i.e., different fluorescence characteristics are strongly affected by interactions with molecules that are located up to several nanometers from the fluorophore).[1] Thanks to the previously mentioned sensitivity, different variants of fluorescence measurements allow monitoring the properties of the host system on the nanometer scale. A number of fluorescence techniques and special probes has been developed that can be used for the evaluation of microviscosity, micropolarity, and local electrostatic potential and for studies of the conformational behavior and transitions in detail.[2] Recently, the use of environment-sensitive fluorescent probes has become more and more popular in biochemistry, colloidal science, and nanoscience (i.e., in research fields dealing with nanostructured systems).[2−6]

One advanced fluorescence technique for studying local properties of nanostructured systems is the solvent relaxation method (SRM).[7−10] This technique probes simultaneously the micropolarity and microviscosity. It is based on the fact that the solvation of a fluorophore in a polar solvent immediately upon excitation is not the optimum one because the absorption of a photon occurs almost instantaneously in comparison with the rate of molecular motion. The surrounding solvent molecules need some time to reorganize and minimize the energy of the excited fluorophore after the change of its dipole moment. The reorganization (relaxation) rate depends strongly on the microviscosity, while the total energy decrease of the excited fluorophore due to the relaxation of the solvation shell translates in the Stokes frequency shift and monitors the micropolarity. Although in nonviscous solvents, a major part of the process occurs in the picosecond time range, the relaxation is generally slowed down in the presence of macromolecules or organized structures in the studied system (e.g., a considerable part of the process proceeds on the nanosecond time scale).[10]

Despite the fact that the solvent relaxation technique is popular in biochemistry and has been frequently used in membrane

* To whom correspondence should be addressed. E-mail: (M.S.) stepanek@natur.cuni.cz or (K.P.) prochaz@vivien.natur.cuni.cz.

(1) Because the term microenvironment is currently being used in the literature, we continued to use it instead of the more appropriate term nanoenvironment.

(2) Bosch, P.; Catalina, E.; Corrales, T.; Peinado, C. *Chem.—Eur. J.* **2005**, *11*, 4313.
(3) Behera, G. B.; Mishra, B. K.; Behera, P. K.; Panda, M. *Adv. Colloid Interface Sci.* **1999**, *82*, 1.
(4) Krishnan, R. V.; Varma, R.; Mayor, S. *J. Fluoresc.* **2001**, *11*, 211.
(5) Epand, R. M.; Kraayenhof, R. *Chem. Phys. Lipids* **1999**, *101*, 57.
(6) Rist, M. J.; Marino, J. P. *Curr. Org. Chem.* **2002**, *6*, 775.
(7) Jarzeba, W.; Walker, G. C.; Johnson, A. E.; Barbara, P. F. *Chem. Phys.* **1991**, *152*, 57.
(8) Hutterer, R.; Schneider, F. W.; Sprinz, H.; Hof, M. *Biophys. Chem.* **1996**, *61*, 151.
(9) Kelkar, D. A.; Chattopadhyay, A. *J. Phys. Chem. B* **2004**, *108*, 12151.
(10) Sýkora, J.; Kapusta, P.; Fidler, V.; Hof, M. *Langmuir* **2002**, *18*, 571.

10.1021/la702277t CCC: $40.75
Published on Web 11/29/2007 PAGE EST: 7.9

research, its use in polymer chemistry is rather limited, although it can yield very unique and detailed information on the structure and dynamics of self-assembled nanoparticles. Recently, SRM has been used for studies of the solvation dynamics of poly(ethylene oxide)-*block*-poly(propylene oxide)-*block*-poly(ethylene oxide) micelles in aqueous media.[11−13] In our laboratory, we have been studying the micellization of block polyelectrolytes and other water-soluble block copolymers by using various fluorescence techniques (both steady-state and time-resolved) in combination with other methods, such as light scattering (LS) and atomic force microscopy, for almost two decades.[14−20] Some time ago, we used SRM for the investigation of the pH-dependent hydration of shells of polystyrene-*block*-poly(2-vinylpyridine)-*block*-poly(ethylene oxide) onion micelles.[20]

Motivation and Aim of the Study. In comparison with the solvent relaxation in isotropic solutions of small molecules, the solvation dynamics, or more precisely the microenvironment relaxation in systems containing nanoparticles, is a very complex process. The system contains relatively large nanoparticles (e.g., polymeric micelles or vesicles with hydrodynamic radii ranging from 10^1 to 10^2 nm), considerably smaller fluorophores with sizes up to several nanometers, and even smaller subnanometer solvent molecules. For studies on the effect of nanoparticles on the behavior of the solvent, the fluorophore has to reside close to the nanoparticle. A suitable probe can be either chemically attached or should have a high affinity to the nanoparticle (i.e., it should strongly adsorb at or solubilize in it). Different nanoparticles have different shapes; the self-assembling copolymers form spherical, ellipsoidal, or rod-like particles, concentric spherical layers, planar sheets, etc. Their properties are generally anisotropic, which complicates the relaxation process and its analysis. Even in the case of highly symmetric spherical micelles and vesicles, the properties of the nanoparticle (density, polarity, and viscosity and of its immediate surroundings) change in the radial direction, which again affects the fluorescence response. Moreover, the positions of individual fluorophores in different nanoparticle systems may differ (e.g., there can exist a fairly broad distribution of distances from the center of a micelle). A considerable (quite common) obstacle for an unambiguous interpretation of the time-resolved Stokes shift is a partitioning of the probe between the core, the shell, and the bulk solvent. The relaxation of the microenvironment in such nanoheterogeneous systems is a very complex process comprised of a number of contributions. The fast contribution corresponds to the reorganization of solvent molecules. Small solvent molecules solvate both the fluorophore and the polymer units. Since the polymer concentration is usually high in the probed region, the polymer units compete with the fluorophore for solvent molecules. In the case of aqueous systems, it is also quite common that the water structure is affected in the immediate proximity of the nanoparticle.[11−13] The motion of solvent molecules is generally slowed down in comparison to the bulk solvent, but the redistribution of solvent molecules is still the fastest process. Another contribution stems from the chain dynamics. We studied systems with a medium polar insoluble PCL block (significantly more polar than, e.g., polypropylene or polystyrene) and a fairly polar PEO block, and therefore, the reorganization of polymer units leads also to the Stokes shift. Because the chain segments are reasonably mobile in swollen systems, the reorganization of polymer segments around the fluorophore results in a response proceeding on the nanosecond time scale. However, in the studied system, one extremely slow process (10^0 −to 10^1 ns) has to be taken into account. This new type of relaxation can be rationalized by the following argument: the aggregates consist of insoluble and soluble parts, and there is a polarity gradient in the radial direction inside each part (especially close to its interface). If the lifetime of the excited state is long enough, some relatively free (adsorbed or solubilized but chemically unattached) excited probes, which are more mobile than polymer segments, can undergo a translation or rotation with respect to the nanoparticle to optimize their interactions with the microenvironment.

Chart 1

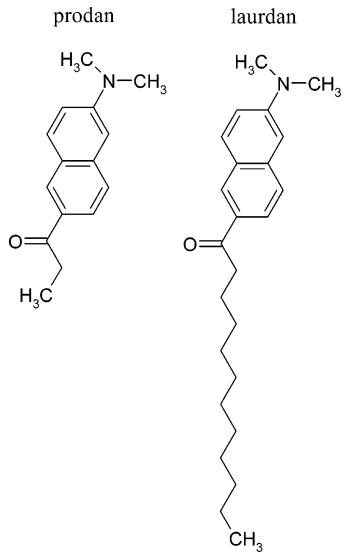

In our previous solvent relaxation dynamics study of polystyrene-*block*-poly(2-vinylpyridine)-*block*-poly(ethylene oxide) onion micelles, PS-PVP-PEO, we found a slow and fairly complicated response due to the relaxation of water molecules solvating the micelle adsorbed fluorophore in polymeric shells.[20] The present work is a continuation of our systematic investigation of the microenvironment relaxation dynamics in systems containing polymeric nanoparticles. We studied the relaxation dynamics in the insoluble part of polymeric vesicles, swollen by an appropriate selective solvent/precipitant mixture (i.e., tetrahydrofurane/H_2O mixture) using nonpolar probes that solubilize in poly(ethylene oxide)-*block*-poly(ϵ-caprolactone) vesicles. Recently, solvent relaxation studies were carried out in microviscous media such as vesicles or sol−gel glasses.[21,22] The authors have shown that 6-propionyl-2-(dimethylamino)naphthalene (prodan) is a suitable probe for this type of research. In this study, we used two probes, (i) prodan and (ii) laurdan[23,24] (Chart 1), that have the same fluorescent portion but differ substantially

(11) Grant, C. D.; DeRitter, M. R.; Steege, K. E.; Fadeeva, T. A.; Castner, E. W. *Langmuir* **2005**, *21*, 1745.
(12) Sen, P.; Ghosh, S.; Sahu, K.; Mondal, S. K.; Roy, D.; Bhattacharyya, K. *J. Chem. Phys.* **2006**, *124*.
(13) Kumbakhar, M.; Ganguly, R. *J. Phys. Chem.* **2007**, *111*, 3935.
(14) Procházka, K.; Bednář, B.; Mukhtar, E.; Svoboda, P.; Trněná, J.; Almgren, M. *J. Phys. Chem.* **1991**, *95*, 4563.
(15) Procházka, K.; Martin, T. J.; Munk, P.; Webber, S. E. *Macromolecules* **1996**, *29*, 6518.
(16) Teng, Y.; Morrison, M. E.; Munk, P.; Webber, S. E.; Procházka, K. *Macromolecules* **1998**, *31*, 3578.
(17) Štěpánek, M.; Procházka, K. *Langmuir* **1999**, *15*, 8800.
(18) Štěpánek, M.; Procházka, K.; Brown, W. *Langmuir* **2000**, *17*, 2502.
(19) Matějíček, P.; Humpolíčková, J.; Procházka, K.; Tuzar, Z.; Špírková, M.; Hof, M.; Webber, S. E. *J. Phys. Chem. B* **2003**, *107*, 8232.
(20) Humpolíčková, J.; Štěpánek, M.; Procházka, K.; Hof, M. *J. Phys. Chem. A* **2005**, *109*, 10803.
(21) Flora, K. K.; Brennan, J. D. *J. Phys. Chem. B* **2001**, *105*, 12003.
(22) Sen, K.; Mukherjee, S.; Patra, A.; Bhattacharyya, K. *J. Phys. Chem. B* **2005**, *109*, 3319.
(23) Parasassi, T.; Krasnowska, E. K.; Bagatolli, L.; Gratton, E. *J. Fluoresc.* **1998**, *8*, 365.
(24) Rowe, B. A.; Neal, S. L. *J. Phys. Chem. B* **2006**, *110*, 15021.

in affinity to the studied nanoparticles due to the absence/presence of a long aliphatic tail. The aim of the study was two-fold: (i) we compare results obtained for both probes and analyze to what extent the partitioning of prodan between vesicles and bulk solvent affects the relaxation and complicates the data analysis and (ii) we present a piece of evidence that the lateral motion of the probe with respect to the nanoparticle within its lifetime is a significant part of the slow relaxation processes in systems containing polymeric nanoparticles.

Experimental Procedures

Materials. Copolymer. The PCL-PEO diblock copolymer with a polydispersity less than 1.4 was purchased from Aldrich. The number-averaged molar masses, M_n, of both PCL and PEO blocks were 5 kg/mol.

Fluorescent Probes. Prodan, 6-propionyl-2-(dimethylamino)-naphthalene, and laurdan, 6-lauroyl-2-(dimethylamino)naphthalene, were purchased from Molecular Probes (Eugene, OR).

Solvents. Tetrahydrofurane and methanol, both luminescence spectroscopy grade, from Fluka and deionized water (specific conductivity lower than 0.5 μS cm^{-1}) were used in the study.

Preparation of Vesicles. The aqueous solutions of PCL-PEO vesicles were prepared according to the following protocol: 30 mg of the copolymer was added to 3 mL of THF (90%)/water mixture and left to shake overnight. Then, the solution was added drop-by-drop to 7 mL of water under vigorous stirring. Finally, the solution was dialyzed extensively against water several times to remove THF completely.

Incorporation of Fluorescent Probes. A total of 25 μL of 0.2 mM prodan stock solution or 10 μL of 0.5 mM laurdan stock solution (both in methanol) was added to 0.8 mL of the PCL-PEO aqueous solution (copolymer concentration, c = 1.55 g/L). After that, we added different amounts of water and THF under vigorous stirring and prepared 2 mL of water/THF (0−30 vol %) solutions in the case of prodan and water/THF (0−50 vol %) solutions in the case of laurdan, in which the concentration of the probe was 2.5 μM. Finally, the samples were left overnight to equilibrate under stirring.

Techniques. LS. The LS setup (ALV, Langen, Germany) consisted of a 633 nm He−Ne laser, an ALV CGS/8F goniometer, an ALV High QE APD detector, and an ALV 5000/EPP multibit, multitau autocorrelator. The solutions for measurements were filtered through 0.45 μm Acrodisc filters. The measurements were carried out for different concentrations (0.4−1.8 g/L) and different angles at 20 °C. The hydrodynamic radii of the vesicles were calculated using the Stokes−Einstein formula from the diffusion coefficients obtained from the second-order cumulant fits of the electric field autocorrelation functions. Details on the LS data evaluation are given in ref 25.

Steady-State Fluorometry. Steady-state fluorescence emission spectra were recorded with a SPEX Fluorolog 3 fluorometer, in a 1 cm quartz cuvette closed with a Teflon stopper. The spectra in the wavenumber domain were fitted to the sum of two log-normal functions[26]

$$S(\omega) = \sum_{i=1}^{2} h_i \exp\left\{-\ln(2)\ln^2\left[\frac{\Delta_i + 2\gamma_i(\omega - \bar{\omega}_i)}{\Delta_i \gamma_i}\right]\right\} \quad (1)$$

where the parameters of the fit h_i, γ_i, $\bar{\omega}_i$, and Δ_i are the peak heights, the asymmetry parameters, the wavenumbers of the peak positions, and the width parameters of the two log-normal subspectra, respectively.

Time-Resolved Fluorometry. A time-correlated single photon counting technique was used for measurements of fluorescence decays at different wavelengths spanning the emission spectra. The decays were recorded on a IBH 5000U time-resolved fluorometer (IBH, Glasgow, U.K.), equipped with an IBH NanoLED-03 excitation source (370 nm peak wavelength, 0.1 ns fwhm of the pulse, and 1 MHz repetition rate) and a cooled Hamamatsu MCP photomultiplier.

The fluorescence decays, $D(t)$, were expressed as triple-exponential functions

$$D(t) = \sum_{i=1}^{3} A_i \exp(-t/\tau_{F,i}) \quad (2)$$

obtained by fitting the experimental data to the convolution of the used model with the instrument response profile, using the Marquardt−Levenberg nonlinear least-squares method. Low values of χ^2 and random distribution of residuals were used as criteria for the quality of the fit.

To analyze the solvent relaxation, fluorescence decays $D(\omega,t)$ measured for various emission wavenumbers ω together with steady-state emission spectra in the wavenumber domain $S(\omega)$ were used to construct the time-resolved emission spectra (TRES) using the formula[26]

$$F(\omega,t) = \frac{D(\omega,t)S(\omega)}{\int_0^\infty D(\omega,t)\mathrm{d}t} \quad (3)$$

The fits of the obtained spectra $F(\omega,t)$ to eq 1 provided time-dependent parameters $h_i(t)$, $\gamma_i(t)$, $\bar{\omega}_i(t)$, and $\Delta_i(t)$.

The parameters of the slow-relaxing subspectrum were used to calculate the correlation function, $C(t)$, allowing us to describe the solvation dynamics occurring in the system

$$C(t) = \frac{\bar{\omega}_1(t) - \bar{\omega}_1(\infty)}{\bar{\omega}_1(0) - \bar{\omega}_1(\infty)} \quad (4)$$

The peak wavenumber at time $t = 0$, which is not directly measurable, was calculated using the simple approximative formula proposed by Maroncelli and Fee[27]

$$\bar{\omega}(0) \approx \bar{\omega}_{e,np} + \bar{\omega}_{a,pol} - \bar{\omega}_{a,np} \quad (5)$$

where the indices np and pol refer to the steady-state peak wavenumbers measured in nonpolar and polar solvents, respectively, and the indices e and a denote the emission and absorption steady-state peak wavenumbers. Eq 5 is valid for emission spectra excited at wavelengths close to the absorption maximum.

Results and Discussion

Characterization of PCL-PEO Vesicles in Water/THF Mixtures by LS. PCL-PEO is an amphiphilic diblock copolymer containing a hydrophobic (water-insoluble) block, PCL, and a hydrophilic (water-soluble) block, PEO. Since water is a strong precipitant for poly(ϵ-caprolactone), PCL-PEO copolymers are not directly soluble in water unless the PCL block is very short. Therefore, the self-assembled nanoparticles have to be prepared indirectly by dissolution of the sample in a mixture of THF with water (rich in THF, which is a good solvent for PCL). In this mildly selective solvent, vesicles (polymersomes) with a relatively thick insoluble PCL middle layer and inner and outer PEO shells are formed. In the next step, the solution was added to an excess of water, and THF was finally removed by dialysis against water. This preparation protocol leads to PCL-PEO vesicles with kinetically frozen PCL domains. The PCL-PEO self-assembly was studied by LS in our recent paper, and the structure of vesicles with a thick insoluble middle layer was further confirmed by atomic force microscopy imaging.[25]

In this study, we investigated the interaction of prodan and laurdan with PCL-PEO vesicles in aqueous solutions and in

(25) Šachl, R.; Uchman, M.; Matějíček, P.; Procházka, K.; Štěpánek, M.; Špírková, M. *Langmuir* **2007**, *23*, 3395.

(26) Horng, M. L.; Gardecki, J. A.; Papazyan, A.; Maroncelli, M. *J. Phys. Chem.* **1995**, *99*, 17311.

(27) Fee, R. S.; Maroncelli, M. *Chem. Phys.* **1994**, *183*, 235.

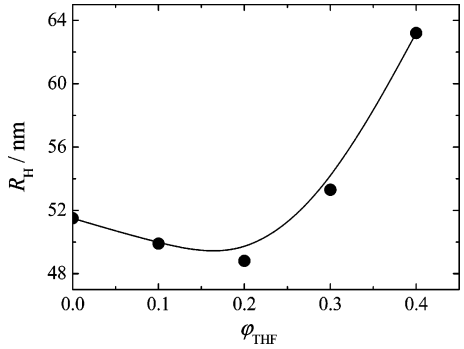

Figure 1. Hydrodynamic radius of PCL-PEO vesicles, R_H, in water/THF solutions as a function of THF volume fraction, φ_{THF}, in the solvent.

mixtures of water with THF. While the basic characterization of PCL-PEO vesicles in aqueous solutions has already been done,[25] the measurement of sizes and aggregation numbers upon the addition of THF has not yet been performed. Hence, the LS study was carried out prior to the fluorescence measurements.

The static LS measurements proved that the aggregation number of vesicles does not change up to 50 vol % of THF. Hence, the observed changes in hydrodynamic radius can be attributed to the swelling/deswelling of individual parts of vesicles. The hydrodynamic radius of vesicles as a function of the THF volume fraction is depicted in Figure 1. Below 20 vol % of THF, the hydrodynamic radius slightly decreases with an increasing amount of THF due to partial collapse of PEO shells. In the region above 20 vol %, the size dependence of vesicles is dominated by the swelling of the PCL layer, and R_H strongly increases with the increasing THF content.

Steady-State Fluorescence Spectra. Since both probes are hydrophobic, one can expect their solubilization in PCL domains in aqueous solutions. When THF is added, (i) the PCL domains swell and (ii) the solubility of hydrophobic probes in the solvent increases. This provokes a partial release of the probe from the core in the bulk solution. Both processes lead to an increase in polarity and a decrease in viscosity of the microenvironment of the probes and influence the microenvironment relaxation. However, a proper discussion of steady-state and time-resolved spectra requires a detailed working hypothesis concerning the localization of probes in individual parts of the nanostructured system and their partitioning between nanoparticles and bulk solvent. The hypothesis, which we are going to confirm by experimental data, is presented next: the partitioning of probes and their localization in different parts of the system is a result of a complicated enthalpy-to-entropy interplay. A probe embedding in the insoluble part is energetically favorable, but it lowers considerably the translational entropy. Its dissolution in the bulk solvent is energetically unfavorable, but the probe gains entropy. From an energy point of view, a localization of the probe in the shell is worse than that in the core but much better than in bulk solvent. From an entropy point of view, the sequence of preferences for this localization is exactly inverse. The actual probe distribution depends on all types of interactions and on the concentration of nanoparticles and the probe. It shifts in favor of the bulk solvent with a decreasing concentration of nanoparticles, and the number ratio of water dispersed/nanoparticle-solubilized probes can be quite important even for fairly hydrophobic probes in purely aqueous media.[18] At low probe concentrations (low loadings), the equilibrium distribution of probes between micellar cores (or insoluble layers in the case of vesicles), shells, and bulk solvent can be described by corresponding partition coefficients, while at high probe concentrations, a saturation limit is reached.[17] The solubilization of hydrophobic probes in shells depends on the chemical nature of the shell forming chains. In our earlier studies,[16,17] we found that solubilization is non-negligible in shells that are formed by annealed electrolytes, such as poly(methacrylic acid), PMA, because water is a bad solvent for their nondissociated chains and they form a distinct hydrophobic layer close to the core. On the other hand, such an effect was never observed in the case of PEO shells.

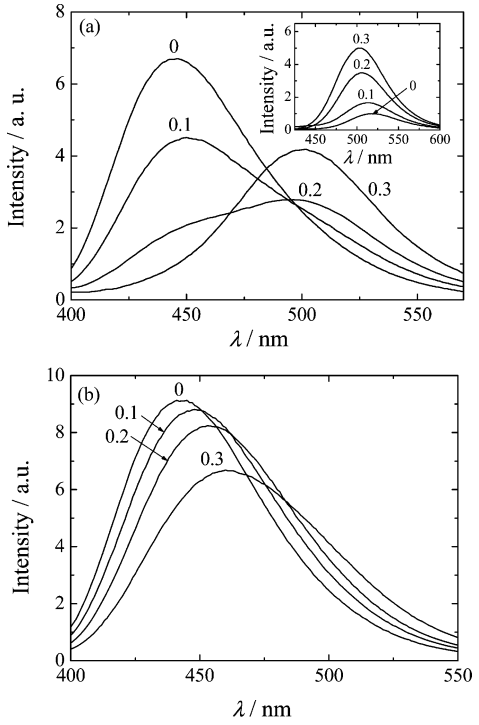

Figure 2. Steady-state emission spectra of (a) prodan and (b) laurdan in the PCL-PEO/water/THF systems. Volume fractions of THF in the water/THF mixed solvent are given as the corresponding spectra. Inset in panel a: steady-state emission spectra of prodan in the water/THF mixed solvent.

The studied nanoparticles are formed by water-insoluble but quite polar PCL and even more polar water-soluble PEO diblock copolymers. Nevertheless, the polarities of polymer blocks are much lower than that of water. Both probes are basically hydrophobic, but they have some amphiphilic character due to the presence of dimethylamino and carbonyl groups. Laurdan contains a long aliphatic chain and is considerably more hydrophobic than prodan. Hence, we assume that the fluorescent headgroups that are identical in both probes are preferentially localized in the PCL/PEO interfacial region and experience a relatively high polarity of the microenvironment (as compared to the polarity of typical nonpolar cores, e.g., of polystyrene cores of currently studied PS-PMA micelles[15−19]). The aliphatic part of the probes is oriented toward the PCL layer. From this assumed localization, we can infer that at low loadings, both prodan and laurdan (the latter in solvents containing enough THF) are distributed predominantly between the PCL/PEO interface and the bulk solvent. In the next two paragraphs, we show that experimental data are consistent with this assumption.

Figure 2 shows the steady-state emission spectra of prodan and laurdan added to PCL-PEO vesicles in different water/THF mixtures. For both probes, the emission maximum wavelength increases with increasing THF content; however, this trend is much less pronounced in the case of laurdan. The difference is caused by the long aliphatic chain of laurdan, which considerably lowers its solubility in THF/water solutions. As a consequence,

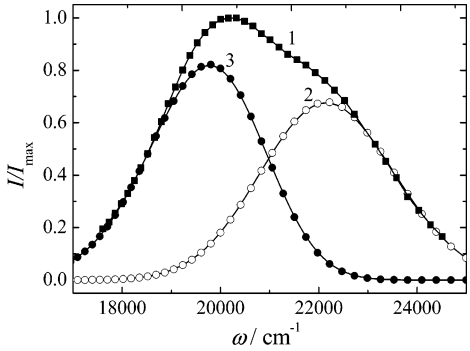

Figure 3. Normalized steady-state emission spectrum of prodan in PCL-PEO/water/THF (20 vol %) system in the wavenumber domain (curve 1) and its subspectra corresponding to the probe at the PCL/PEO interface (curve 2) and in bulk solution (curve 3).

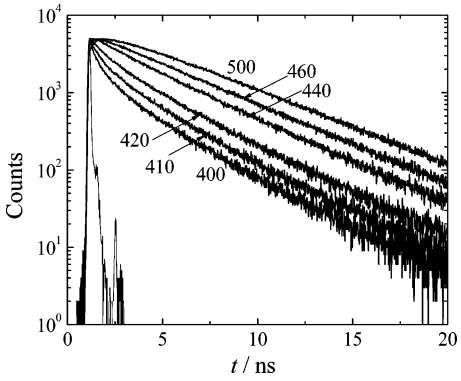

Figure 4. Emission decays of laurdan in PCL-PEO aqueous solution. Emission wavelengths in nanometers are given at the corresponding decay curves.

Table 1. Results of Fits of Emission Decays of Laurdan in PCL-PEO Aqueous Solution[a]

λ (nm)	A_1	A_2	A_3	$\tau_{F,1}$ (ns)	$\tau_{F,2}$ (ns)	$\tau_{F,3}$ (ns)	χ^2
400	0.117	0.057	0.038	0.11	0.71	2.98	1.109
410	0.081	0.053	0.058	0.19	0.95	3.13	1.158
420	0.046	0.054	0.076	0.27	1.25	3.48	1.087
440	−0.009	0.041	0.118	0.11	1.87	3.99	1.096
460	−0.038	−0.018	0.169	0.13	0.62	4.18	1.095
500	−0.062	−0.076	0.222	0.24	1.45	4.53	1.020

[a] Parameters of triple-exponential fits of the decays (eq 2) and χ^2 values.

only a small fraction of laurdan molecules escapes from PCL domains in bulk as compared to prodan. We assume that the change in the laurdan emission spectrum is mainly due to swelling of PCL domains by THF, which makes the microenvironment of the probe more fluid and accelerates the overall relaxation. Hence, the steady-state spectrum in THF-containing solutions reflects the behavior of more relaxed states. In contrast to laurdan, a considerable amount of prodan is released to the bulk solution upon addition of THF, and the observed emission spectrum contains the contributions from prodan molecules in a polar environment (in the bulk solution and in PEO shells) and in PCL hydrophobic domains. This is especially evident at the spectrum in the solution containing 20 vol % THF, which is clearly bimodal (Figure 2a, curve 0.2). In PCL-PEO/water/THF (30 vol %), the bulk solvent subspectrum already dominates the emission. The emission spectra of prodan in pure water and water/THF mixtures (without PCL-PEO vesicles) are shown for comparison in the inset in Figure 2a. Both the quantum yield and the emission maximum wavelength reflect the decrease in polarity with increasing content of THF ($\epsilon_{water} = 80.1$ at 20 °C and $\epsilon_{THF} = 7.5$ at 22 °C[28]). The fact that the wavelengths of the emission maxima of prodan and laurdan in pure aqueous solutions of the vesicles are almost identical confirms our assumption that the headgroups of both probes are localized in similar microenvironments close to the PCL/PEO interface.

In principle, the prodan spectrum can be decomposed in two log-normal components, and the fraction of the prodan emission from polar and nonviscous media, predominantly from the bulk solvent, can be calculated as the ratio of the pertinent subspectrum area to the area of the whole spectrum. In practice, however, the fitting procedure is hindered by a low contribution of one of the two subspectra (either the red-shifted one or the blue-shifted one) to the overall emission. (We tried to improve the resolution by varying the excitation wavelength in the region from 320 to 370 nm, but the corresponding changes in the emission spectra were negligible.) Only the PCL-PEO/water/THF (20 vol %) system where both emissions have comparable intensities provides reasonable results. The knowledge of the prodan spectrum in bulk solvent allows us to reduce the number of the fitted variables; for the description of the solution subspectrum, we can use all parameters that we obtained from the log-normal fit for prodan in the water/THF (20 vol %) mixture, except the height.

A decomposition of the prodan emission spectrum for the PCL-PEO/water/THF (20 vol %) system is shown in Figure 3. The subspectrum corresponding to the emission of prodan embedded in the vesicles (curve 2 in Figure 3) has a maximum at 22 000 cm^{-1} (450 nm), slightly red-shifted as compared to the prodan emission in pure aqueous PCL-PEO systems (445 nm) due to the swelling of PCL domains by THF, which increases their polarity and fluidity. The fraction of the emission corresponding to prodan in the bulk solvent, F, can be calculated as the ratio of the solution subspectrum (curve 3 in Figure 3) area to the area of the whole spectrum. For the PCL-PEO/water/THF (20 vol %) system, $F = 0.71$. It is necessary to keep in mind that this value does not correspond to the molar fraction of bulk-solubilized prodan due to different quantum yields of the probe in the PCL domain and in the bulk solution.

Time-Resolved Fluorescence Measurements. To monitor differences in the dynamics of the microenvironment relaxation of prodan and laurdan in PCL-PEO vesicles, we measured the fluorescence emission decays of both probes in solutions with an increasing content of THF at different wavelengths. (Typical results of the decay measurements are shown in Figure 4 for the laurdan emission in PCL-PEO aqueous solution. The values of amplitudes, A_i, and fluorescence lifetimes, $\tau_{F,i}$, obtained from the fits of the decays shown in Figure 4 are summarized in Table 1, together with the corresponding χ^2 values.) The time-resolved emission spectra were then constructed from the steady-state spectra and the fits of the decays using eq 3.

Figure 5 shows the normalized time-resolved emission spectra of prodan the PCL-PEO/water/THF (10 vol %) system. The spectra recorded in early times after excitation are composed of two well-separated subspectra. While the shift of the blue subspectrum (23 300 cm^{-1} at 0.01 ns after excitation) corresponding to the emission of prodan molecules in hydrophobic domains is clearly visible in the monitored time range, the position of the emission maximum of the red subspectrum (20 000 cm^{-1} at 0.01 ns) does not change, and this emission disappears in the shoulder of the blue one in later times because the relative intensity of the red subspectrum decreases due to a shorter lifetime of prodan in the bulk solution. The subspectra can be obtained from

(28) Lide, D. R. *CRC Handbook of Chemistry and Physics*; CRC Press: Boca Raton, FL, 1995; pp 6-159−6-192.

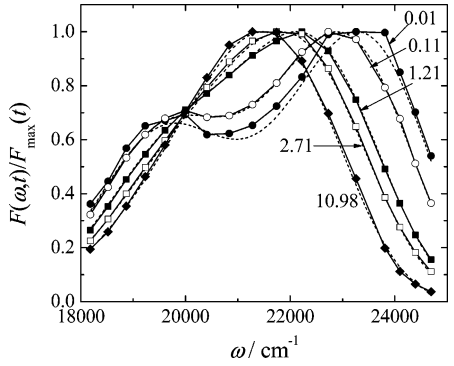

Figure 5. Normalized time-resolved emission spectra of prodan in the PCL-PEO/water/THF (10 vol %) system at various times after excitation (the values, in ns, are given at the corresponding curves) and fits of the spectra to eq 1 (dashed curves).

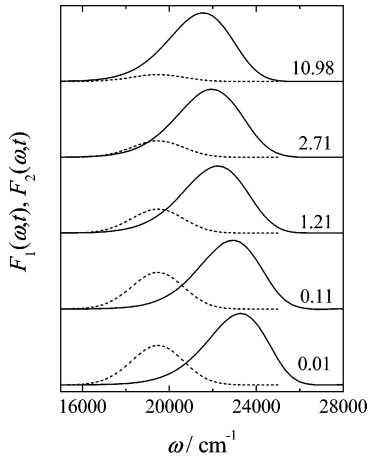

Figure 6. Log-normal components of the fits from Figure 5. The values at the curves are times after excitation in nanoseconds.

the fit of the time-resolved spectra to eq 1 (the fitted functions are shown in Figure 5 as dashed lines).

The results of the fitting procedure for individual time-resolved spectra (i.e., the log-normal components of the fits) are plotted in Figure 6. It is evident that the relaxation of the red subspectrum is so fast that a substantial part of the nonviscous polar solvent reorientation is accomplished prior to the first measurement, that is, 0.01 ns after excitation, and no further relaxation process is observed, unlike in the case of prodan in a highly viscous environment of the polar PCL core. The estimate of the time zero spectra according to Maroncelli and Fee[27] indicates that the unresolved part is rather small in aqueous systems but that it increases with the amount of added THF.

In the previous section, we have shown that the decomposition of the steady-state spectra of prodan in PCL-PEO/water/THF solutions is difficult if one of the two overlapping subspectra dominates. Figure 5 suggests that the problem of the resolution can be substantially suppressed by using the time-resolved spectra instead of the steady-state one: since the lifetime of prodan in the bulk solution (and in the PEO shell as well) is much shorter as compared to that in the PCL domain, the contribution of the red subspectrum to the overall prodan emission is much larger in the time-resolved spectra recorded in early times after excitation than that in the steady-state spectrum, which facilitates the decomposition of the spectrum.

Figure 7 shows the first recorded time-resolved spectra (at 0.01 ns) of prodan in PCL-PEO/water/THF systems. The relative intensities of the red subspectra strongly increase with an increasing content of THF as the solubility of prodan in the bulk

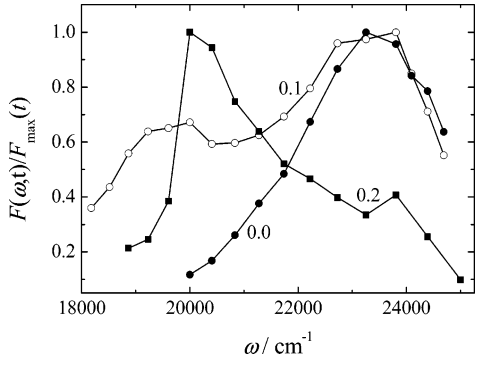

Figure 7. First recorded time-resolved emission spectrum ($t = 0.01$ ns after excitation) of prodan in the PCL-PEO/water/THF systems. Volume fractions of THF in the water/THF mixed solvent are given at the corresponding spectra.

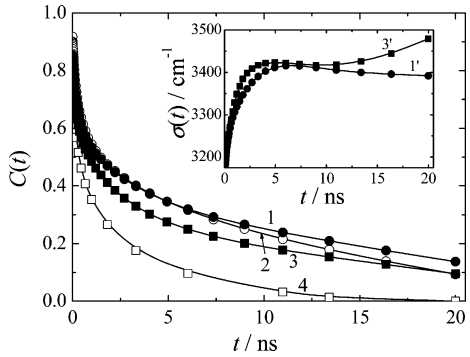

Figure 8. Correlation functions, $C(t)$, for laurdan and prodan blue subspectrum emissions in the PCL-PEO/water system (curves 1 and 2, respectively) and for the laurdan and prodan blue subspectrum emissions in the PCL-PEO/water/THF (10 vol %) system (curves 3 and 4, respectively). Inset: fwhm, $\sigma(t)$, for laurdan blue subspectrum emissions in the PCL-PEO/water and PCL-PEO/water/THF (10 vol %) systems (curves 1′ and 3′, respectively).

solvent increases. The maxima of the red subspectra are shifted to higher wavenumbers in solutions with higher contents of THF due to decreased polarity of the bulk solvent. On the other hand, the emission maximum of the blue component does not almost change because of its slow relaxation with respect to the time of the measurement.

Previously, we have shown that the bimodal time-resolved spectra can be decomposed in a quickly relaxing red subspectrum and a slowly relaxing blue subspectrum. The former subspectrum corresponding to probes in the bulk solvent is fully relaxed within the time window of our experimental method, and we focus only on the latter one (i.e., on the slowly relaxing blue component of probes embedded in the PCL/PEO interfacial region of polymeric nanoparticles). The comparison of correlation functions, $C(t)$, of the blue subspectra of laurdan (curves 1 and 3) and prodan (curves 2 and 4) in PCL-PEO/water and in PCL-PEO/water/THF (10 vol %), respectively, is shown in Figure 8.

The experimental correlation functions in systems containing nanoparticles have generally the form of multiexponential decays with several components needed for a satisfactory fit. The corresponding relaxation times, τ_i, characterize the rates of individual contributions to the relaxation process. Even though we focus only on the relaxation of the blue subspectrum, its time response is still complex because individual relaxation modes (i.e., motion of small molecules and polymer segments) are mutually correlated. Therefore, it is not possible to ascribe individual experimental relaxation times to well-defined physical motions. In this work, we characterize the experimental correlation functions by (i) mean relaxation time, τ_R, and (ii) two time

Table 2. Characteristics of Correlation Functions of Prodan and Laurdan Blue Subspectrum Emissions in PCL-PEO Solutions[a]

	C_0	C_1	τ_1 (ns)	C_2	τ_2 (ns)	τ_R (ns)
prodan, water	0.067	0.518	8.16	0.318	0.29	5.35
laurdan, water	0.127	0.443	7.28	0.278	0.32	5.69
prodan, 10% THF	0.009	0.478	3.19	0.351	0.17	1.85
laurdan, 10% THF	0.112	0.440	5.05	0.269	0.26	4.53

[a] Relaxation times and pre-exponential factors obtained by double-exponential fitting of the correlation functions, $C(t) = C_0 + C_1e^{-t/\tau_1} + C_2e^{-t/\tau_2}$, and the mean relaxation times, τ_R.

components, τ_1 and τ_2, obtained from the fit: $C(t) = C_0 + C_1e^{-t/\tau_1} + C_2e^{-t/\tau_2}$. The mean relaxation time characterizes the ensemble average effective microviscosity of the medium surrounding the fluorophore. Its advantage consists of the fact that it provides a simple and comprehensive integral characterization of the system. Further, it is well defined and can be evaluated with a sufficient precision according to the following formula:

$$\tau_R = \int_0^\infty C(t)dt \quad (6)$$

The τ_R values and the results of double-exponential fits for the $C(t)$ functions in Figure 8 are listed in Table 2. In the case of prodan emission, the addition of THF causes a substantial decrease in τ_R. In the case of laurdan, which is more strongly bound to the PCL domain, the average relaxation time shortens only slightly with increasing THF content due to the decrease in viscosity of the PCL domain swollen with THF. It is evident that the observed trends of mean relaxation times provide a qualitatively correct picture of the system behavior. The interpretation of double-exponential fits provides a more detailed description of the process. The most obvious and fairly straightforward difference between prodan- and laurdan-labeled systems consists of the effect of THF on the slow (unresolved) part of the relaxation, which is expressed by the coefficient C_0. For prodan, this coefficient is low (0.067) in the purely aqueous system and drops almost to zero (0.009) after a 10% THF addition, while for laurdan, C_0 is 0.127 in pure water and drops only a little to 0.112 after the addition of THF (i.e., a non-negligible contribution of the slow relaxation persists in the swollen PCL domain). The pre-exponentials, C_1 and C_2, are similar in both systems and do not change much with the THF content, but both the long and the short relaxation times, τ_1 and τ_2, respectively, are lower and decrease more with THF content for the prodan-labeled than for the laurdan-labeled system.

The observation that not only the steady-state but also the time-resolved spectra can be satisfactorily decomposed into two sets of subspectra (instead of three) provides support of our simplifying assumption that the distribution of probes in the studied system can be explained by their partitioning between the PCL/PEO interfacial region and bulk solvent is, in principle, correct. A careful inspection of correlation functions together with the analysis of shapes of time-resolved spectra containing different amounts of THF allows us to propose a more detailed description of the relaxation process. A comparison of curves for both probes suggests that the lateral motion of prodan in vesicles contributes to the overall relaxation. In this work, we focus on the nanosecond region, where we monitor the behavior of the microenvironment of probes bound to micelles. The time-dependent Stokes shift of the blue subspectrum monitors the behavior of the microenvironment of the fluorescent part of the bound prodan, which is the same as that in laurdan. If the observed relaxation was only a result of the redistribution of solvent molecules and PCL segments around the fluorescent group, the relaxation rates and hence the time-dependent curves for both probes in the same solvent mixture (i.e., under the same swelling of the PCL domain) should be similar. However, the correlation function decays considerably more slowly for laurdan than for prodan under the same conditions, and a significantly higher THF content in the laurdan-labeled system is necessary to obtain comparable mean relaxation times. Close to the PCL/PEO interface, the micropolarity changes strongly in the radial direction, and a small displacement of the probe results in non-negligible changes in electrostatic interactions. Hence, the lateral motion of the probe contributes to the energy minimization. The results suggest that the PCL swelling in a 10 vol % THF aqueous mixture enables the motion of prodan but is not sufficient to liberate the motion of laurdan, which has a higher affinity to PCL than prodan because it is effectively anchored by its aliphatic tail. The electrostatic force generated after the change of the dipole moment is not sufficient to provoke the energy minimizing motion of the anchored probe within the lifetime of the excited state. One can argue that the localization and distributions of individual probes across the PCL layer may differ. Laurdan could be embedded slightly deeper in the PCL layer (one can imagine that it is pulled inside by its aliphatic chain) than prodan and since the microviscosity gradient in the interfacial region is steep, the relaxation of the microenvironment would be slowed down. However, we have shown that the emission maxima wavelengths of both probes in pure aqueous solutions of the vesicles are almost the same in the steady-state and also in the first recorded time-resolved spectra, indicating the same polarity of the environment of prodan and laurdan headgroups. Because not only the gradient in microviscosity but also that in micropolarity is steep close to the PCL/PEO interface, the spectra suggest a very similar location of headgroups in both cases. As concerns the THF-containing systems, the swelling of the PCL layer is more or less homogeneous, and possible differences in the distribution of fluorophores cannot explain large differences in the amounts of THF necessary for a comparably fast responses of prodan and laurdan, either.

Several research groups studied recently the behavior of fluorophores in solvent mixtures and found a relatively slow dynamics due to preferential solvation and redistribution of solvent molecules in the solvation shell upon a sudden change of the dipole moment of the probe after its transfer to the excited state.[29−31] The relaxation was found to proceed on the time scale of tens of nanoseconds in the 1,4-dioxane (DOX)/water mixtures and more slowly in alkane-alcohol mixtures, where the components differ considerably in polarity. In our system, the preferential solvation can affect mainly the behavior of the red-shifted subspectrum. Because the studied THF/water sytem is similar to the DOX/water system and the viscosity of THF is lower as compared to DOX, we assume that this process occurs on the subnanosecond time scale, which is just at the resolution limit of our experimental setup. This is (together with the fact that the intensity of the red subspectrum decreases quickly with time) the main reason as to why we do not observe this process.

Because the PCL domains are swollen by solvent, a contribution of the redistribution of solvent molecules around the excited fluorophore does certainly play a role also in the time response of the blue subspectrum. Nevertheless, the really slow and well-pronounced part of the time-resolved Stokes shift in the region

(29) Cichos, F.; Willert, A.; Rempel, U.; von Borczykowski, C. *J. Phys. Chem. A* **1997**, *101*, 8179.
(30) Molotsky, T.; Huppert, D. *J. Phys. Chem. A* **2003**, *107*, 8449.
(31) Mukherjee, S.; Sahu, K.; Roy, D.; Mondal, S. K.; Bhattacharyya, K. *Chem. Phys. Lett.* **2004**, *384*, 128.

exceeding 10 ns cannot be explained by the dynamics of solvent molecules only.

Besides the $C(t)$ function, also the fwhm, $\sigma(t)$, of the time-resolved emission spectrum provides important pieces of information on the relaxation process. The fwhm can be calculated as follows:

$$\sigma(t) = \Delta_1(t) \frac{\sinh \gamma_1(t)}{\gamma_1(t)} \quad (7)$$

The higher the $\sigma(t)$ values are, the more heterogeneous the population of the excited states that emit at a given time t is (i.e., $\sigma(t)$ reflects the heterogeneity in the microenvironment of various excited probes). In homogeneous systems (e.g., in nonviscous solutions), the half-width attains the maximum almost immediately upon excitation and decreases with time. In heterogeneous systems, the time dependence of fwhm is not monotonous. It increases at early times because not only varying numbers of fluorophores in differently relaxed states contribute to the overall emission but also the spatial heterogeneity of the microenvironment contributes to the transient increase of the disorder of the system. This type of behavior applies also to nanoheterogeneous systems because the spatial sensitivity and therefore the spatial resolution of the relaxation method correspond to the nanometer scale. Assuming that the relaxation time is shorter than the excited-state lifetime (i.e., that we monitor the relaxation process from the beginning (except the subnanosecond region) to its end), the half-width, $\sigma(t)$, passes a maximum and later decreases because the contribution from the fully relaxed states to the spectrum prevails at late stages of the relaxation process. The detailed analysis of the influence of the probe site heterogeneity on the emission line-width time dependence is given in the review article by Richert.[32]

The inset in Figure 8 shows the fwhm for the laurdan emission in PCL-PEO/water and PCL-PEO/water/THF (10%) (curves 1′ and 3′, respectively). The initial increase in the $\sigma(t)$ function is steeper for the PCL-PEO/water/THF (10%) system because the relaxation is faster due to a lower viscosity of the THF-swollen PCL domain. The decreasing parts of the curves are only a little pronounced in both cases, which suggests that the emission lifetime of the fluorophore is too short to monitor the whole relaxation process. Moreover, in the case of the water/THF (10%) solution, we observed a further increase in fwhm at times higher than 10 ns after excitation. Since laurdan molecules can move in the PCL domain swollen with THF, we assume that this increase reflects a change in the microenvironment polarity due to the relocation of the probes close to the PCL/PEO interface during the lifetime of the excited state. It is noteworthy that a nonnegligible increase is observed for prodan even in a nonswollen PCL-domain (i.e., in the PCL-PEO solution in pure water), which suggests that the movement of laurdan in the PCL domain is hindered mainly due to the presence of its long aliphatic chain. The study shows that the $\sigma(t)$ plots provide useful information on systems with probes distributed in different media. Their unexpected shapes can, at least, indicate that the relaxation proceeds as a very complex process. We are persuaded that a superficial evaluation of the half-width in the case of a multimodal (or a shoulder containing) spectrum is not correct. The spectrum should be decomposed in all potential time-resolved contributions (which is not always possible), and the time evolution of their maxima positions and of their half-widths should be evaluated separately and discussed in detail. Only such a complicated approach would enable the extraction of individual relaxation times that can be unambiguously ascribed to physically meaningful relaxation modes.

(32) Richert, R. *J. Chem. Phys.* **2000**, *113*, 8404.

Conclusion

The steady-state and time-resolved fluorescence spectroscopy study of the solubilization and relaxation dynamics of prodan and laurdan (the probes that have the same fluorescent headgroup and differ considerably in length of the aliphatic portion) in solutions of diblock copolymer vesicles of PCL-PEO in water/THF mixtures of varying compositions revealed that both probes solubilize efficiently in the compact PCL layer of the PCL-PEO vesicles (close to the PCL/PEO interface) in purely aqueous media. After the addition of 20−30 vol % of THF, laurdan remains located in insoluble parts of vesicles because it contains a long hydrophobic aliphatic tail and is effectively anchored in the PCL domain, while prodan is partially released in the bulk solvent mixture.

The partitioning of prodan between the compact (even though swollen) and quite viscous PCL/PEO interfacial region and the polar media of low viscosity complicates the relaxation process and hinders considerably its accurate analysis. The time-resolved emission spectra have to be decomposed in appropriate time-dependent components and treated separately. We believe that the outlined approach reveals important details and helps to explain the details of the relaxation dynamics. Nevertheless, extreme caution is needed when data in similar complex systems are interpreted at the molecular level.

An important piece of knowledge was obtained from the comparison of the behavior of probes that have the same fluorescent headgroup and differ substantially in the length of the aliphatic portion. The results provide a new piece of evidence for our assumption that in complex systems containing large nanoparticles, medium fluorophores, and small solvent molecules, not only the reorganization of solvent molecules and polymer units around the fluorophore but also a lateral motion (and possibly also rotation) of the probe with respect to the nanoparticle contribute significantly to the relaxation process. The last mentioned motion is reflected by the slow part of the process (in the studied systems, it corresponds to 10^0 to 10^1 ns).

Acknowledgment. K.P. acknowledges financial support from the Ministry of Education of the Czech Republic (Long-Term Research Project MSM0021620857), the Grant Agency of the Academy of Sciences of the Czech Republic (Grant IAA401110702), and the Marie Curie Research and Training Network (Grant 505027, POLYAMPHI). M.H. acknowledges financial support from the Grant Agency of the Academy of Sciences of the Czech Republic (Grant IAA400400503).

LA702277T